Evaluation of the Seismic Performance of Circular and Interlocking RC Bridge Columns under Bidirectional Shake Table Loading

Juan G. Arias-Acosta
Power Transmission Division of Siemens, Erlangen, Germany

David H. Sanders
University of Nevada, Reno, USA

SUMMARY:
Evidence found after significant earthquakes have shown that the force and deformation capacity of reinforced concrete bridge columns (RCBC) can be significantly affected by the combined effect of dynamic loads (axial, shear, bending and torsion); these load combinations can seriously affect the seismic performance of bridges resulting in unexpected large deformations and extensive damage. To study the impact of different loadings combinations on both circular and oblong sections (double interlocking spirals), eight scaled cantilever-type RCBC specimens were tested on the bidirectional shake table facility at the University of Nevada, Reno (UNR). As part of the study, a unique inertial loading system was developed to allow shake table testing of single columns under biaxial ground motions. Two sets of circular and interlocking specimens were subjected to different levels of biaxial, torsion and vertical loads through real time earthquake motions. The performance of the specimens was assessed in terms of strength, deformation, and failure mode.

Keywords: bridge engineering, reinforced concrete columns, bidirectional shake table test, combined loadings,

1. INTRODUCTION

Earthquake loadings induce complex combinations of forces and deformations to bridge structures. These interactions are caused by, among other reasons, spatially-complex variation of earthquake ground motions, the bridge structural configurations and the interaction between input and response characteristics. As a result, the seismic behavior of reinforced concrete bridge columns (RCBC) will be seriously affected, and that in turn influences the performance of bridges as essential components of transportation systems.

In order to address the complex behavior of RCBC under combined loadings and to develop a fundamental knowledge of the impact of combined actions on column performance and their implications on system response through analytical and experimental research, a comprehensive project sponsored by the National Science Foundation was established that included researchers from six U.S. institutions.

The component research at the University of Nevada, Reno (UNR) was focused on the development of refined analysis and shaking table tests of large scale cantilever-type models of RCBC typical of bridges in California subjected to different levels of biaxial, torsion and vertical loads through real time earthquake motions. The experimental study was divided into two stages; first specimens were tested without axial load and subsequently, other set of identical specimens were tested including axial load and P-delta effects. The seismic performance of the specimens was assessed in terms of strength, deformation, and failure mode. These results will be used to validate analytical tools, developing new inelastic models for RCBC under combined loadings and to propose new design methodologies. This paper highlights the experimental investigation.

2. SPECIMENS AND MASS SETUP

Four 1/3 scale specimens with circular section and four ¼ scale specimens with oblong section were designed and constructed using current details typical of bridges in California in accordance with the Seismic Design Criteria (CALTRANS, 2006). The structural configurations were similar to previous columns tested at UNR under unidirectional shake table loading (Laplace et al., 1999 and Correal et al., 2004). The height of the columns was set to 1830 mm (72 in) and the specimens' aspect ratio was selected to allow for flexural dominated behavior.

For circular columns the diameter of the specimens was 406 mm (16 in), thus the aspect ratio was 4.5. The columns were reinforced with 20 No.4 (D13) deformed longitudinal bars, distributed evenly around the perimeter and fully developed with 90 degree hooks in the footing. The confinement consisted of a continuous spiral made from galvanized smooth steel wire with a diameter of 6.25 mm (0.25 in) and a pitch of 38 mm (1.5 in). The clear cover was set to 19 mm (0.75 in) and the longitudinal and volumetric transverse reinforcement ratio were 2% and 0.92%, respectively. Reinforced concrete footings and loading top heads were designed to attach the specimens to the shake table floor and to connect the inertial mass system to the specimens, respectively. Details of specimens are shown in Fig. 1.a.

For oblong columns the width of the short side was 305 mm (12 in), while that in the long side was 445 mm (17.5 in). The longitudinal reinforcement consisted of 32 No. 3 (D10) deformed bars, spaced evenly in two interlocked circular patterns and fully developed in the footing. The resulting reinforcement ratio was 2%, while the volumetric ratio of the spiral reinforcement was 1.0%. The confinement consisted of two continuous spirals made from galvanized smooth steel wire with a diameter of 4.9 mm (0.192 in) and a pitch of 25 mm (1.0 in). The clear cover was set to 13 mm (0.5 in). Since oblong columns were reinforced with double interlocking spirals they are called hereinafter as interlocking columns. Details of the interlocking columns are shown in Fig. 1.b.

The compressive strength of the concrete was set as 30 MPa (4.5 ksi), while the nominal yielding strength of the steel was 447 MPa (64 ksi) for deformed bars and 420 MPa (60 ksi) for wire. Table 1. summarizes the real properties of steel and concrete based on coupons and cylinders.

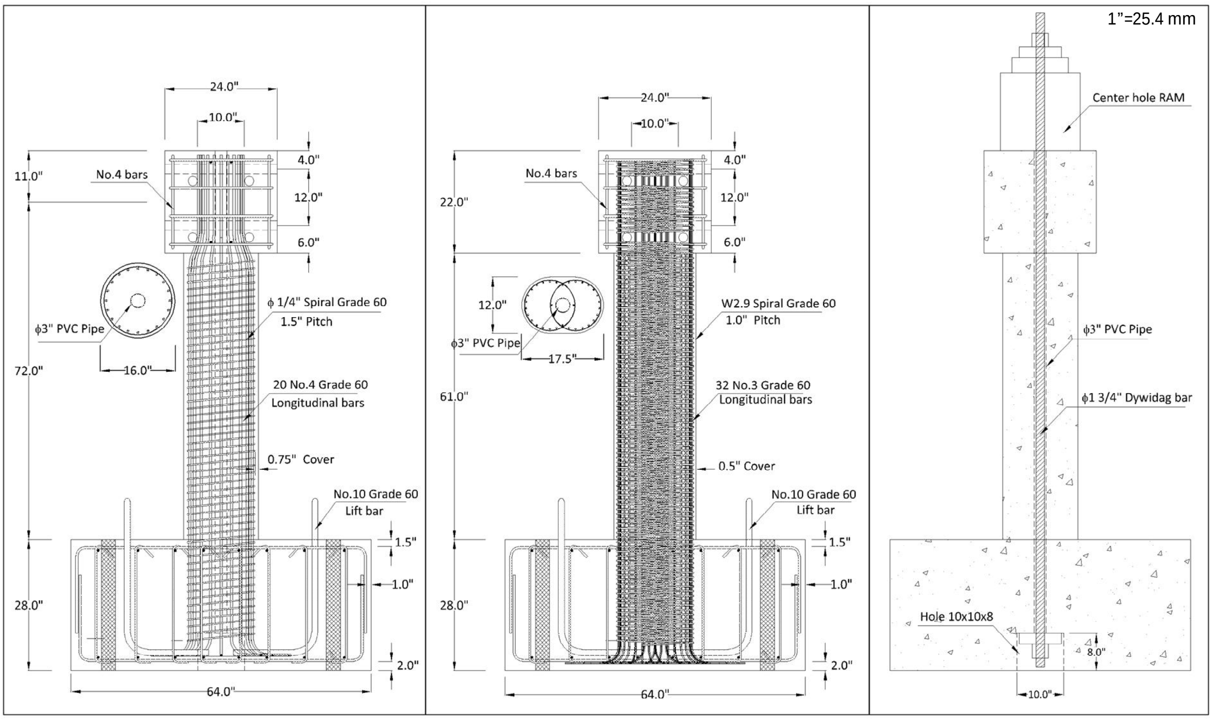

a) Circular b) Interlocking c) Axial load system

Figure 1. Geometric configuration and reinforcement for the RCBC specimens

Table 1. Material Properties

Test day	Concrete Compressive Strength [MPa]			
	Circular (C)		Interlocking (I)	
Column	**Footing**	**Column**	**Footing**	**Column**
1	39	32	42	39
2	41	32	43	31
3	48	40	43	42
4	48	42	48	50

Steel Properties	No.3	No.4	W2.9	W5.0
Yield stress [MPa]	423	448	400	400
Yield strain	0.0022	0.0023	0.0024	0.0024
Strain at hardening	0.012	0.0075	N.A	N.A
Peak stress [MPa]	653	712	541	541
Strain at peak	0.124	0.115	0.115	0.126
Fracture stress [MPa]	561	687	537	484
Fracture strain	0.195	0.151	0.154	0.138

As part of the study, a unique inertial loading system named the Bidirectional Mass Rig (BMR) was developed to enable the shake table test of single RCBC under biaxial motions. The setup was designed to provide a supporting structure that carries safely the vertical component of the inertial mass (superstructure weight) but allows transfer of the inertial forces from the structure to the specimen, when the shake table and specimen move together.

The mass setup is composed by a 3D four columns steel frame and a moving platform that sits on ball bearings located at the top of the columns. The platform is connected to the specimen through links in two perpendicular directions, which allow transferring of shear and torsion but not axial load (Fig. 2a). Additional mass is set on the platform to simulate a portion of the bridge superstructure weight, and this can be placed in a symmetric or asymmetric configuration to induce different levels of torsion. The superstructure mass was set as 356 kN (80 kips), which is approximately 0.08Agf'c, were f'c is the compressive concrete strength, and Ag the gross section of the column.

For specimens with axial load, a compressive load was applied directly to the specimen through a center-hole ram equipped with a servo-valve. The ram was connected to the specimens throughout an unbonded prestressed bar placed in an ungrouted conduit in the middle of the column and anchored in the footing as it is illustrated in Fig. 1c. The prestressed bar was to induce the required level of axial load in the columns rather than increases its displacement capacity as has been found in other studies (Sakai *et al.*, 2006).

Since the BMR does not induce secondary moments (P-delta effects) in the specimen and the unbonded prestressed bar inside the column would generate restoring lateral forces, additional dynamic actuators were located at the top of the specimen to induce the equivalent force to have P-delta effects and to compensate the restoring force (Fig. 2b).

In view of the complexity of the system in terms of the active control of dynamic actuators, the test program was divided in two phases. At the beginning a set of two circular and two interlocking columns were tested without any axial load or P-delta effects (Phase I). A second phase incorporated all the effects. Table 2 outline the test matrix for the entire research project.

Table 2. Experimental test matrix

Test	Specimen	Shape Diameter (mm)	Scale	Ht (mm)	Biaxial Bending	Torsion	Axial & PD-effect
Phase I	C1	406	1:3	1830	✓	Low	Not Considered
	C2	406	1:3	1830	✓	Moderate	Not Considered
	I1	305x445	1:4	1830	✓	Low	Not Considered
	I2	305x445	1:4	1830	✓	Moderate	Not Considered
Phase II	C1-P	406	1:3	1830	✓	Low	Considered
	C1-P	406	1:3	1830	✓	Moderate	Considered
	I1-P	305x445	1:4	1830	✓	Low	Considered
	I2-P	305x445	1:4	1830	✓	Moderate	Considered

A sophisticated control procedure was developed to drive simultaneously the shake table and the dynamic actuators through hybrid simulation. In this procedure, the dynamic actuators were accurately controlled by force using active feedback and actuator compliance, as well as a calibrated spring-pack between the actuator and the column head. The target time history equivalent force was determined from analytical simulations of single cantilever columns subjected to biaxial earthquake loading and including P-delta effects and prestressed tendons.

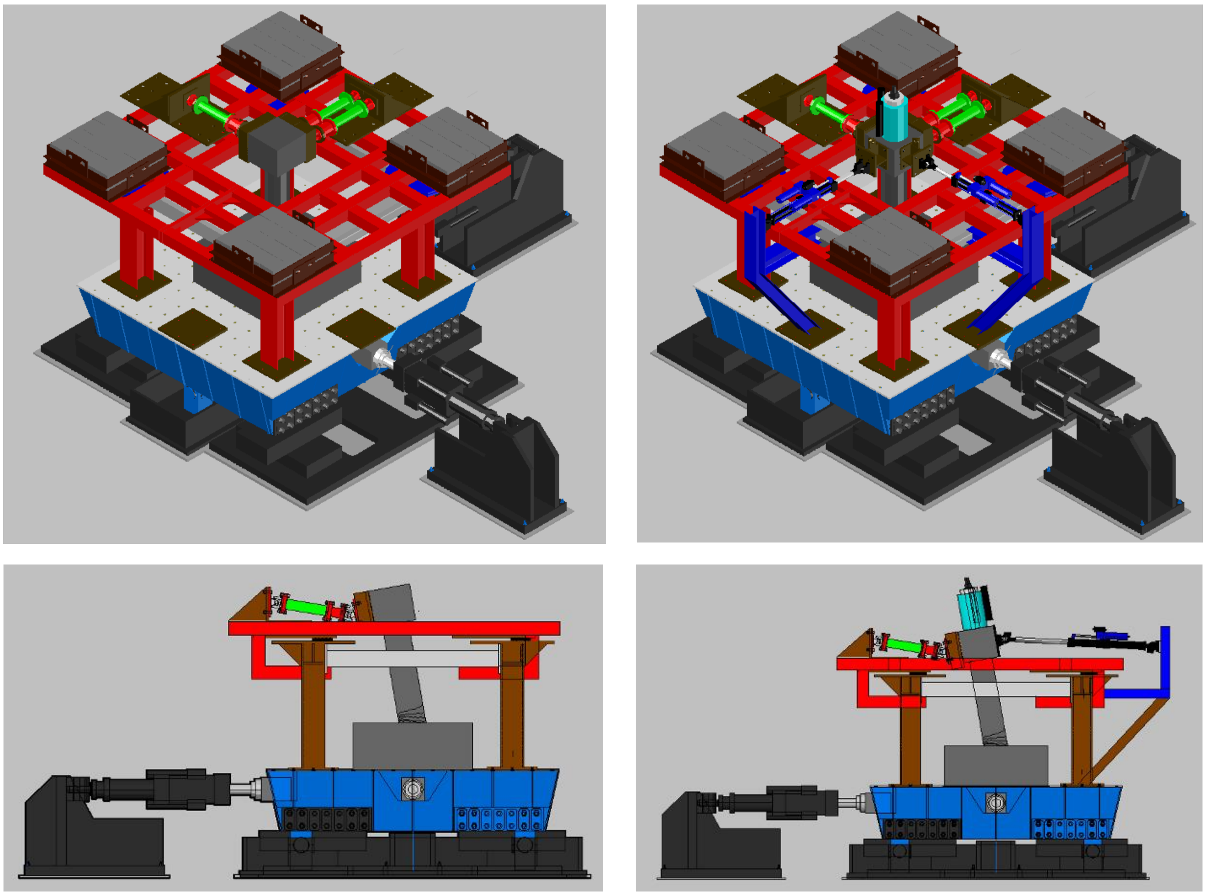

a) Without axial load. b) With axial load (prestressed bar + actuators)

Figure 2. Inertial loading system (Bidirectional Mass Rig)

3. PRELIMINARY ANALYSIS AND EARTHQUAKE SELECTION

In order to determine suitable input loadings to be used during the tests and to anticipate the seismic performance of the specimens and test setup, analytical simulations were conducted using OpenSees (Mazzoni et al.,2006). Analytical models of either single cantilever-type specimens or models of the specimens including the inertial loading system were studied under different levels of earthquake excitations and mass distribution to determine limit states in the behavior of the specimens during the tests.

Different analytical approaches were used to anticipate the biaxial flexural behavior of the specimens. Nonlinear beam-columns with uniaxial fibers were used to simulate the biaxial flexural behavior of the columns. The stress-strain properties of the unconfined and confined concrete were simulated using Mander's model (Mander et al., 1988). Similarly, the longitudinal reinforcing steel was idealized using the uniaxial steel material model developed by Chang and Mander (1994). The actual strength of the concrete measured from cylinders and the stress-strain backbone curve measured from coupons were used as the input parameters for the steel and concrete models. Also, the reinforcement slippage was included in the models in the form of additional rotation at the plastic hinge location. Since inelastic fiber models for torsion are still under development (Mullapudi et al., 2008), a reduction factor of 20% of the elastic torsional stiffness (GJ) was used to take in account the torsional degradation of the concrete in agreement with the Seismic Design Criteria (CALTRANS, 2006).

From the results of single cantilever columns tested under uniaxial shake table loading at UNR (Laplace et al., 1999 and Correal et al., 2004), it was found that the specimens modeled using beam-with-hinges, bond-slip, strain rate effects, viscous damping and a combination of Concrete07 and ReinforcingSteel materials in Opensees, provided the best estimation of the measured performance.

To estimate the lateral load-displacement capacities and the deformation characteristics of the specimens, moment-curvature and pushover analyses were performed first. To account for biaxial bending in the sectional analyses, capacity orbits were calculated by considering variations in the orientation of the neutral axis (NA). A modification of the Mander's model for confined concrete was required to get ultimate curvatures in agreement with previous experimental results. The modification consisted of the addition of a straight line connecting the points of crushing strain and corresponding strength with a strain of two times the crushing strain at zero strength. Table 3 summarizes the biaxial capacities of the circular and interlocking specimens for each direction of analysis. Once the capacities were estimated, series of nonlinear time history analysis were conducted. For that, different cases of mass distribution were studied to determine the largest bending and torsional demands on the specimens.

Table 3. Lateral load capacities of the specimens

Circular Columns, NA @ 45°		
Properties	**P=0**	**P=356 kN**
ϕy	0.00032	0.00032
My (kN-m)	165	202
ϕu	0.0057	0.0046
Mu (kN-m)	214	234
$\mu\phi$	17.8	14.5
$\mu\Delta$	7.32	6.01
Vu (kN)	117	128

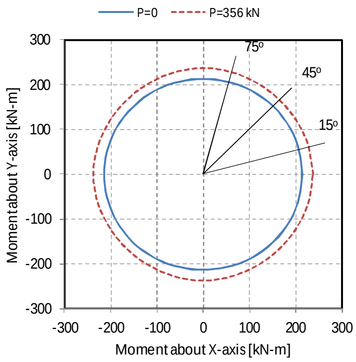

Interlocking Columns				
Properties	**Short dimension , NA @ 0°**		**Long dimension, NA @ 90°**	
	P=0	**P=356 kN**	**P=0**	**P=356 kN**
ϕy	0.00038	0.00039	0.00028	0.00029
My (kN-m)	120	148	170	214
ϕu	0.0107	0.0079	0.0059	0.0048
Mu (kN-m)	159	176	222	251
$\mu\phi$	28	20	21	16
$\mu\Delta$	10	7.9	7.6	6.6
Vu (kN)	87	96	121	139

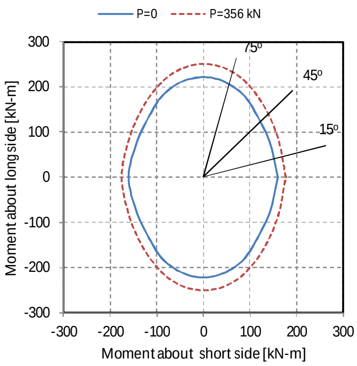

For the preliminary analysis the two horizontal components of the 1940 Imperial Valley earthquake at El Centro, the 1992 Petrolia at Mendocino, and the 1994 Northridge at Sylmar earthquakes were used as the input motions. Scale factors were applied to the records in order to get acceleration demands representative of design and maximum considered earthquakes in California. These scale factors were successively increased until the maximum capacity of the analytical model was achieved. Also, the time axis of the input motions was scaled using the square root of the scale, then, factors of 0.58 and 0.5 were used for circular and interlocking specimens, respectively. From the preliminary dynamic analysis, it was found that the record Petrolia at Mendocino (PET) and Sylmar at Northridge (SYL) amplified by a factor of 1.8 induced the maximum displacement ductility demand on the circular and double interlocking specimens without exceeding the shake table capacity.

4. TEST PROCEDURE

The circular specimens were subjected to the two components of the Petrolia record, whereas the interlocking ones were subjected to the Sylmar motion. Two identical circular (C1, C2) and two identical interlocking columns (I1, I2) were biaxialy excited without applying axial force, while a similar set of circular (C1-P, C2-P) and interlocking (I1-P, I2-P) specimens were identically tested but dynamic actuators were added to apply the axial load and biaxial lateral forces to simulate P-delta effects. The only difference between specimens 1 and 2 was the way in which the mass was distributed on the BMR; for specimen 1 a symmetric distribution of masses was used, while it was asymmetric for specimens 2. Hence, for the later specimens more torsion was expected.

Each column was subjected to the selected earthquakes increasing the amplitude in successive runs. Small intensities (10% to 20% of the real earthquake) were initially applied to determine elastic properties and the effective yielding, subsequently, the amplitude of the records was successively increased until failure. Failure was defined as the rupture of either the longitudinal or transverse steel or the point when the shake table or BMR physical limits were reached and a higher amplitude motion could not be applied. Signals of white noise were applied to the specimens to measure the change in period and damping ratio between runs. The maximum accelerations imposed in both horizontal directions to the shake table were 0.9g and 1.2g, for Petrolia and 1.1g and 1.5g for Sylmar ground motion. These accelerations corresponded to an amplification factor of 1.8 times the selected earthquakes.

The specimens were extensively instrumented to monitor the local and global response. Electrical transducers were used at selected locations to measure acceleration, lateral force and displacement, torsion, and curvature. Furthermore, strain gages were attached to the longitudinal and transverse steel to measure local deformations. For the specimens of the first phase of testing, sensors were placed inside the concrete to measure the variation in strains at different locations by a team from the University of Houston lead by Dr. Y.L Mo (Gu et al., 2010). For the second phase of testing, in addition to the electrical transducers, an optical 3D measurement coordinate system (Krypton system) was used to measure the displacements of the specimens in a 3D space. After each run of the test protocol, the damage was documented by marking cracks and taking a number of pictures.

5. EXPERIMENTAL RESULTS

5.1. Observed Behavior

The behavior of the specimens was controlled by the biaxial effect of bending, with horizontal cracks distributed over the specimen height, as well as some inclined cracks at the plastic hinge region near the column base. For small amplitude runs some horizontal flexural cracks were seen on the lower half of the columns and were distributed around the perimeter of the specimens. The first bar yielding for all the specimens was observed between 40% and 60% of the applied shake table motions (PET for circular and SYL for interlocking). The damage at this stage was characterized both by the increase in horizontal and the presence of inclined cracks. The first concrete spalling was observed around 100% of the earthquakes. At this point a large number of horizontal and inclined cracks were observed on the specimens. The spirals and longitudinal bars were visible after 140% of the motions. The failure of the specimens was observed for accelerations levels exceeding 160% of the actual earthquakes. The specimens failed after a plastic hinge was fully developed at the column base; the failure mechanism was initiated by buckling of longitudinal bars, followed by reinforcement rupture and degradation of the concrete core. For specimen C2-P a premature failure occurred due to malfunctioning of the shake table control system at 140% PET. Figure 3 shows the final damage state for all the columns. From the figure it is evident that less cracking was observed for the specimens of phase II; this was attributed to the compressive axial load which limited the level of tension in the concrete. For these specimens it was also observed that P-delta effects resulted in a faster stiffness degradation that influenced the failure of the specimens.

Figure 3. Damage on the specimens after failure

5.2. Measured Behavior

The cumulative force-displacement hysteresis curves and the displacement orbits for the specimens are shown in Figs. 4 and 6. The displacements in each direction were calculated by subtracting the table displacement from the top column displacement, whereas the force was recorded from the load cell placed in the links. The hysteresis response were typical of columns with flexure dominate behavior in which stable loops and progressive reduction in lateral stiffness is observed up to the maximum force is reached. After that point a sudden change in the specimens occurred due to the longitudinal bars buckling and rupture.

From Fig. 4 it is clear that the hysteresis for the circular specimens showed a biased motion in one direction that became more significant after subsequent runs. This effect was due to the ground motion, which is considered as a near fault record with asymmetric peak velocity pulses. As a consequence of this effect, large residual displacements were observed during the test. On the other hand, from the displacement orbits it was evident that the displacement component followed a line with an inclination of approximately 30^o.

For the interlocking specimens the hysteresis in the long direction showed a symmetric pattern with almost the same maximum displacement in each direction. Similarly, in the short direction the motion was symmetric but just until the maximum force was observed, after that the behavior was influenced by residual displacements (Fig. 6). The displacement orbits showed that the displacement trajectories of the specimens were highly dominated by displacements on the long side of the columns.

Figures 5 and 7 show the base moment-drift envelopes for the tested specimens. The behavior of specimen sets was almost the same, nevertheless a slightly less capacity was observed for specimens with torsion (C2 and I2) after the first yielding. This behavior is explained because less concrete is effective to resist the tensile stresses in the longitudinal bars induced by the combination of torsion and bending deformations. This effect was more important at high intensity runs and played a significant role in the failure mechanism of the specimens as seen in Fig. 3.

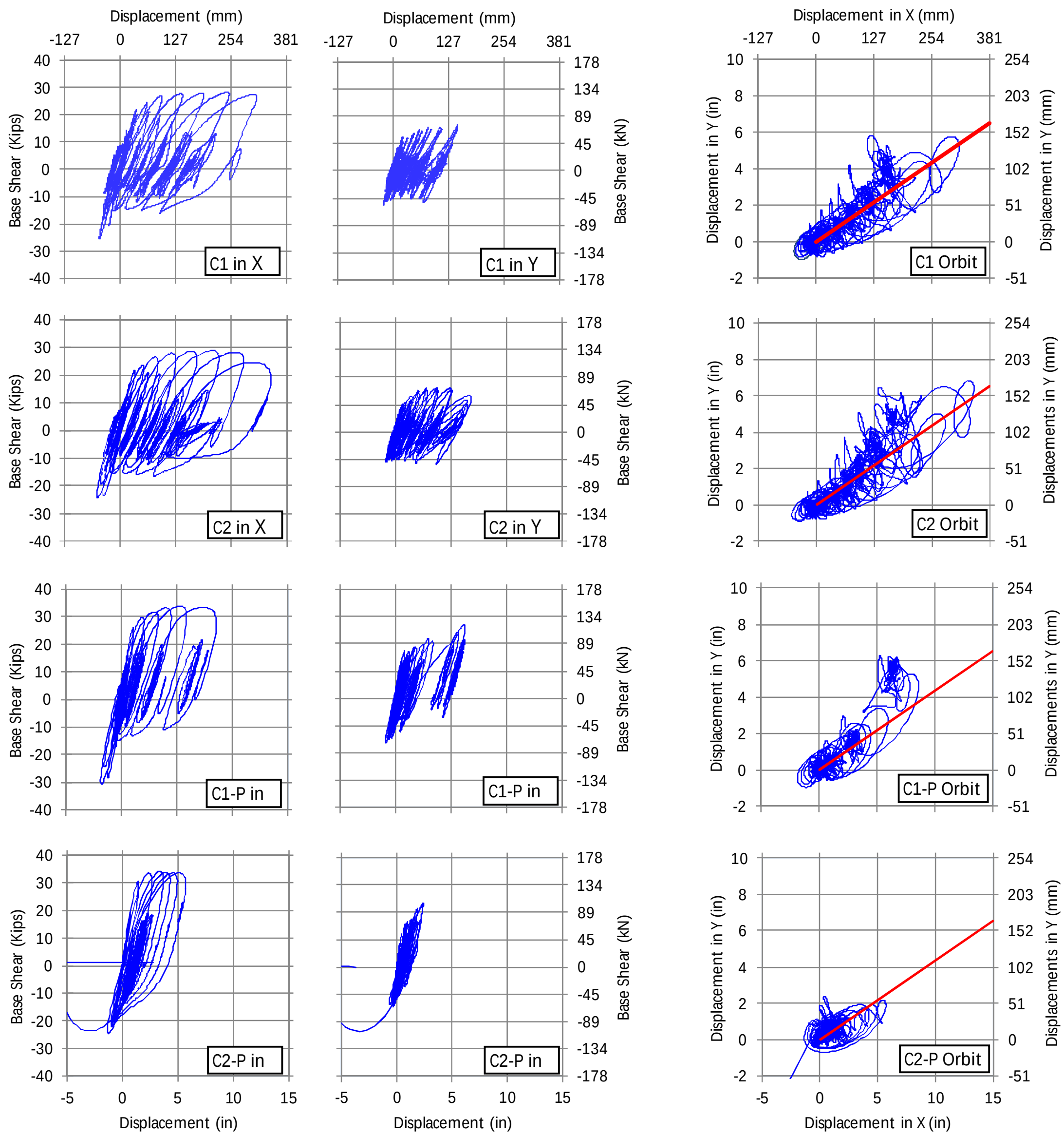

Figure 4. Force-displacement hysteresis for circular column

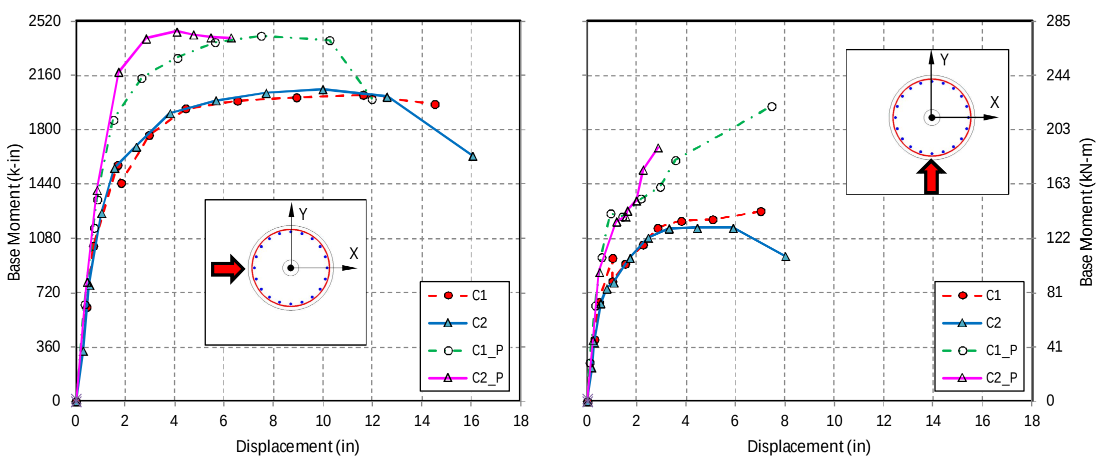

Figure 5. Base Moment-drift envelopes (Circular specimens)

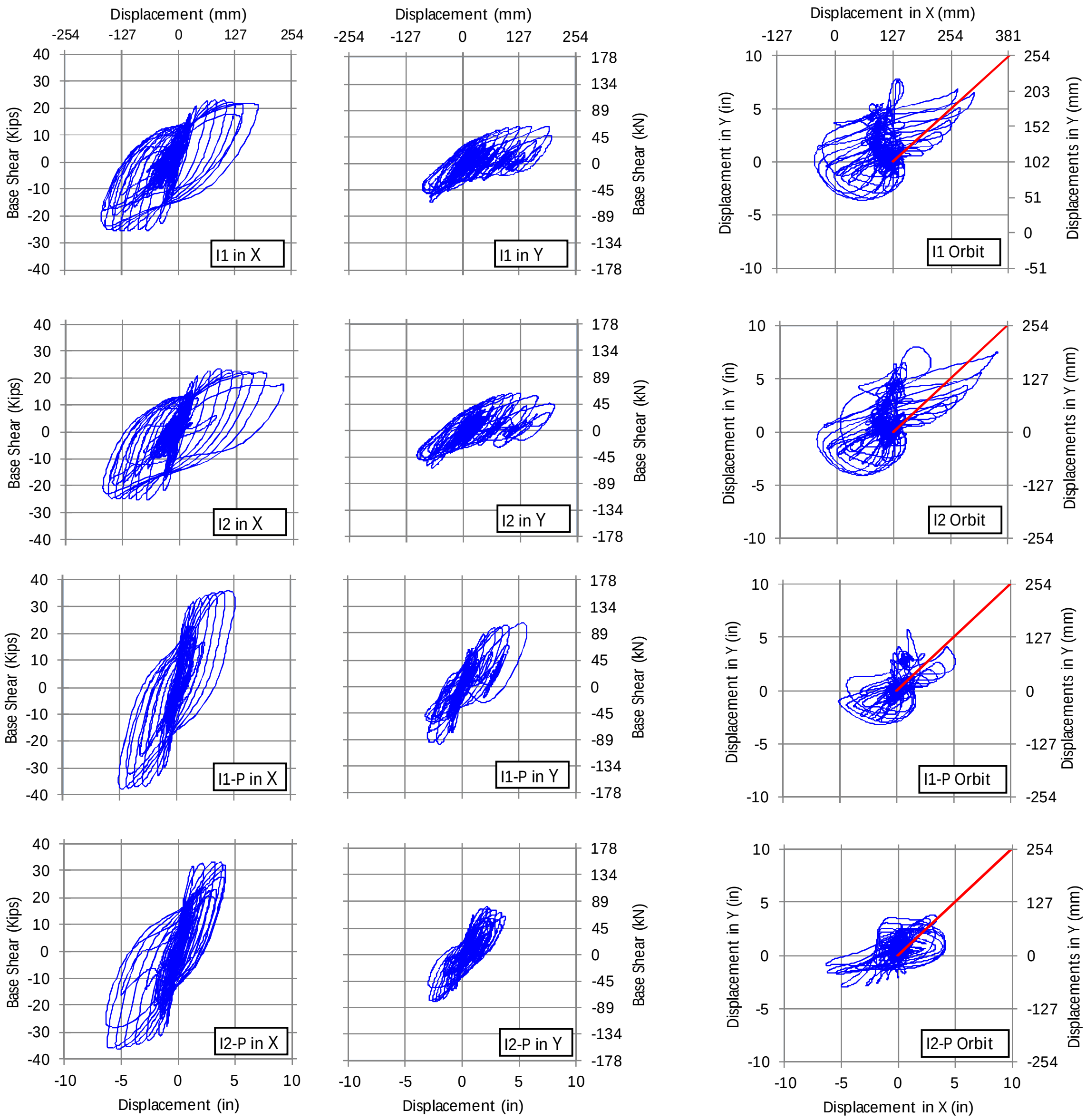

Figure 6. Force-displacement hysteresis for interlocking columns

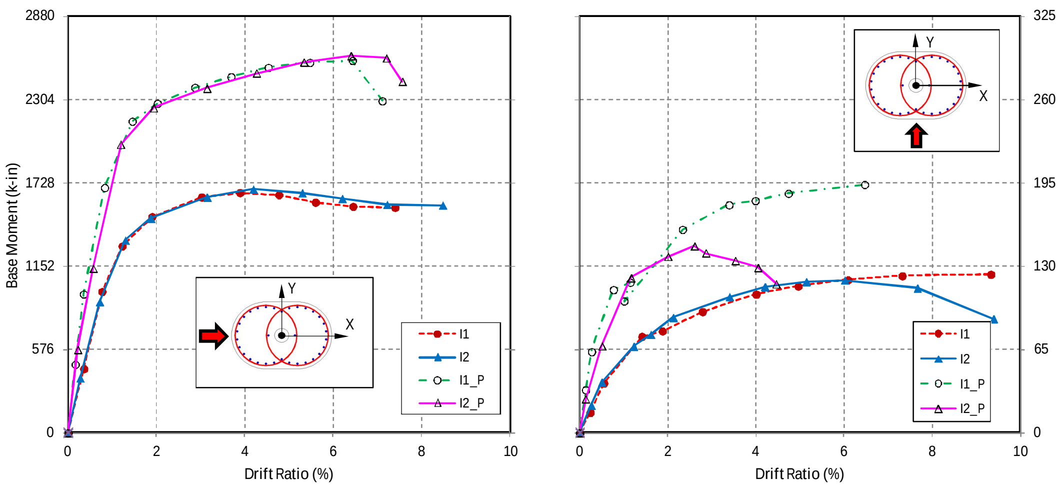

Figure 7. Base Moment-drift envelopes (Interlocking specimens)

6. CONCLUSIONS

The new inertial mass system used on bidirectional shake table tests at UNR represent a significant advance in the simulation of single RCBC under simultaneous loads induced by real time earthquake motions. One of the most important characteristics of this system is that it allows the interaction between bending and torsion with or without axial load. Furthermore, the low friction ball bearings allow transferring of inertial loads, even under low levels of lateral excitations.

For the sections and ground motions used in this study, the biaxial interactions affected mostly the seismic performance of the columns along the direction where the small component of the earthquake was applied (Y direction). It was observed that the lateral capacity along the transverse direction was reduced in comparison to the values calculated from moment-curvature analyses, whereas for the longitudinal direction the measured capacity was in good agreement with the calculated one, indicating that the seismic response in this direction was only slightly affected by the behavior in the transverse direction. The asymmetric mass configuration used for specimens C2, I2, C2-P and I2-P only induced low values of torsion on the columns. The softening of the column's torsional stiffness due to the formation of the plastic hinge limited the development of the torsion.

For all the specimens of phase I, it was observed that after yielding, the maximum lateral capacity remained almost constant for increasing earthquake intensities until the longitudinal bar buckling occurred. After this point the response was characterized by a pronounced stiffness and capacity degradation, leading to failure. Similar behavior was observed for the specimens of phase II, where the axial compression increased the lateral capacity but at the same time, the ultimate behavior was notably affected by stiffness degradations and P-delta effects, making the specimens more susceptible to lateral instability.

ACKNOWLEDGEMENTS
The research presented in this paper was funded by NEESR-SG-0530737 under support from the National Science Foundation (NSF) through the National Earthquake Hazards Reduction Program (NEHRP). The assistance of Ian Buckle, Patrick Laplace, Steven Kenny, Chad Lyttle and the staff of the George E. Brown, Jr. Network for Earthquake Engineering Simulation (NEES) Site at University of Nevada Reno is gratefully acknowledged.

REFERENCES

California Department of Transportation, 2006. Bridge Design Specifications, Engineering Service Center, Earthquake Engineering Branch, California, USA, 250 pp.

Chang, G. and Mander, J., 1994. Seismic Energy Based Fatigue Damage Analysis of Bridge Columns: Part I – Evaluation of Seismic capacity, *NCEER Technical Report 94-0006.*

Correal, J.F., Saiidi, M.S., and Sanders, D.H., 2004. Seismic Performance of RC Bridge Columns Reinforced with Interlocking Spirals, *Report No. CCEER-04-6*, Center for Civil Engineering Earthquake Research, Department of Civil Engineering, University of Nevada-Reno, USA, 438 pp.

Gu, H., Moslehy, J., Sanders, D., Song, G. and Mo, L., 2010**.** Multi-functional Smart Aggregate-based Structural Health Monitoring of Circular Reinforced Concrete Columns Subjected to Seismic Excitations. *Smart Materials and Structures*, 19 (06).

Mander J.B., Priestley, M.J.N. and Park, R., 1988. Theoretical Stress-Strain Model for Confined Concrete, *Journal of Structural Eng*., 114 (8), pp 1804-1826.

Laplace, P., Sanders, D.H., and Saiidi, M.S., 1999. Shake Table Testing of Flexure Dominated Reinforced Concrete Bridge Columns, *Report No. CCEER-99-13*, Center for Civil Engineering Earthquake Research, Department of Civil Engineering, University of Nevada-Reno, USA, 438 pp.

Mazzoni, S., McKenna, F., Scott, M., and Fenves, G.L., 2006. Open System for Earthquake Engineering Simulation (OpenSees), *User manual*, version 1.7.3, Pacific Earthquake Engineering Research Center, University of California, Berkeley, California, USA.

Mullapudi, T.R., Ayoub, S. and Belarbi, A., 2008. Effect of Coupled Shear-Bending Deformations on the Behavior of RC Highway Structures Subjected to Extreme Seismic Loading, *Proceedings of the 6th National Seismic Conference on Bridges & Highways*, Paper No. P19, Charleston, South Carolina, USA.

Sakai, J., Jeong H. and Mahin, S.A., 2006. Reinforced Concrete Bridge Columns that Re-Center Following Earthquakes, *Proc. of the 8th U.S. National Conference on Earthquake Engineering*, Paper No. 1421, CA.